Geophysica (1987), Vol. 23, No. 1, pp. 59–77
Printed in Finland

551.511:551.465.7(261.24Øresund)

MARINE METEOROLOGICAL CONDITIONS AND AIR-SEA EXCHANGE CHARACTERISTICS DURING THE »ØRESUND» EXPERIMENT

by

J. LAUNIAINEN (1), H. GRÖNVALL (2) and J. VAINIO (2)

Abstract

Marine meteorological observations made on board a research vessel during the intensive period (4.–9. June 1984) of the Øresund-84 experiment, are reported. Most of the time, the atmospheric surface layer was stably stratified, the turbulent air-sea fluxes were rather small and, the sea surface temperature was higher on the upwind (Swedish) side than on downwind (Danish) side. Accordingly, the over-water surface wind speed and the flux of momentum turned out to be smaller at the downwind stations than at the upwind stations. The upwind water vapour flux was larger as well, whereas, in the sensible heat flux areal differences were not so apparent. Due to higher sea surface temperature near the Swedish coast the stability was less stable on the upwind side.

1. *Introduction*

During May and June 1984 an extensive field experiment, the Øresund-84 experiment (see GRYNING, 1985), was carried out in the Sound area between Denmark and Sweden (55°45′N, 12°45′E) as a Nordic co-operation, organised by NORDFORSK (Nordic Co-Operative Organization for Applied Research). The goal of this mesoscale dispersion experiment was primarily to gain meteorological, marine meteorological and oceanographic data for investigation of atmospheric turbulence and dispersion in conditions modified by air-sea and coastal land-sea interaction.

During the intensive period of the project, from 4 to 9 June 1984, marine meteorological observations in the area were made on board a Finnish research vessel

(1) Department of Geophysics, University of Helsinki, Fabianinkatu 24 A, 00100 Helsinki, Finland.

(2) Finnish Institute of Marine Research, Box 33, 00931 Helsinki, Finland.

»Aranda». In addition to versatile marine meteorological observations, also oceanographic observations were made, connected with studies of water exchange between the Baltic Sea and the North Sea. This paper reports the observation activity and the data as well as outlines the marine meteorological characteristics and the air-sea interaction in the area during the period.

As to the weather and meteorological conditions, the intensive period of the project was carried out during later conditions of a long-lasting spring high in the northern and northeastern Scandinavia and a weak low in the southwestern Baltic Sea and Denmark area. This resulted in a warm weather in the whole Scandinavia and light easterly or northeasterly winds in the research area.

2. *Data*

2.1 Observations

The observational sea area, bounded by the Danish city Copenhagen and the Swedish cities Malmö and Landskrona, is shown in Fig. 1. The observations were made by cruising continuously day night in a grid system of 5 observation points.

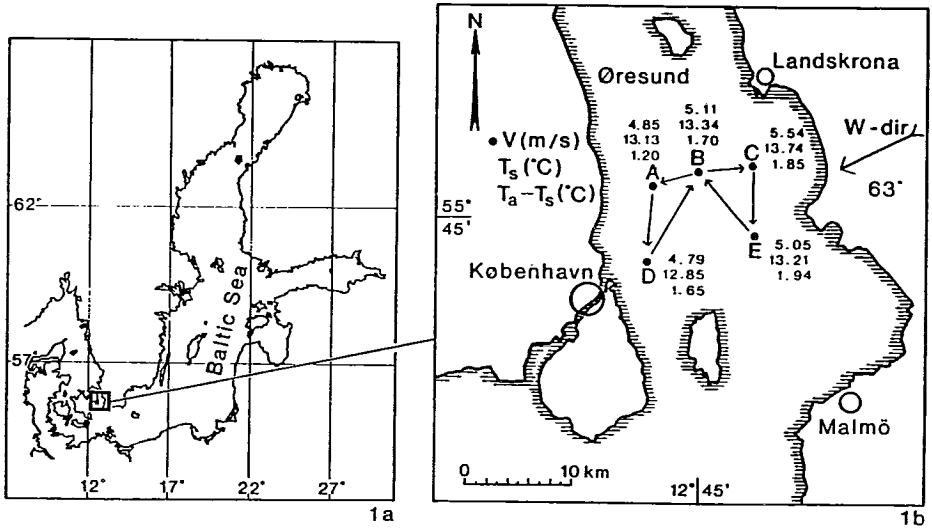

Fig. 1. Research area and location of observation stations. Arrows show the ship's cruising pattern. The upper number in Fig. 1.b gives the average wind speed, the middle one gives the mean sea surface temperature and the lowest one gives the mean air-sea temperature difference during the intensive period of 4th to 9th June 1984. W-dir gives the (vectorial) mean wind direction for the period.

For each observation point the ship was stopped and turned against the wind. The total observation period at a station was most frequently one hour, consisting of six consecutive observation periods, 10 min. each. The cruising time (distance) between the stations was about one hour and thus, the central station B (*cf.* Fig. 1) was visited 3 to 5 times, whereas the other stations were visited 2 to 3 times a day, (*cf.* Appendix 2).

The observation quantities, observing instruments and observation accuracies are given in Table 1, and the location of the sensors on board is shown in Fig. 2. A special bow sprit was used in order to avoid interference of the ship's hull with the wind and temperature measurements. For calculation of the humidity quantities, dry and wet bulb temperatures were measured by an artificially ventilated

Table 1. Observation quantities on board R/V Aranda. The symbols refer to the data given in the figures and in Appendix 2.

Quantity	Obs. height from SL	Location on board	Observing instrument	Resolution/ accuracy of a single measur.	Notes
Wind direction	10.8	front mast	wind vane	10°	inst measurem at the end of 10 min obs. period
Wind speed, V	8.2	bow sprit	cup anemom dist const 1.19 m	0.1 m/s	10 min average before the observation time given
Max wind speed	8.2	bow sprit	»	»	max gust (of 2 s) during 10 min obs. period
Wind speed	10.8	front mast	»	»	10 min average
Air temperature, T_a	8.2	bow sprit	Pt-500 resistor	better than 0.1°C	
Dry air temp. T_d	10.8	front mast	Pt-500	»	artificially ventilated measuring screen
Wet bulb temp. T_w	10.8	»	»	»	»
Sea surface temp. T_s (CTD)	−0.1		»	0.01°C	CTD-sond
Sea surface temp. (radiometric)	0.0		radio-metric		
Vertical temp. profile in water				0.01°C	CTD-sond
Salinity profile				0.01 ‰	CTD-sond

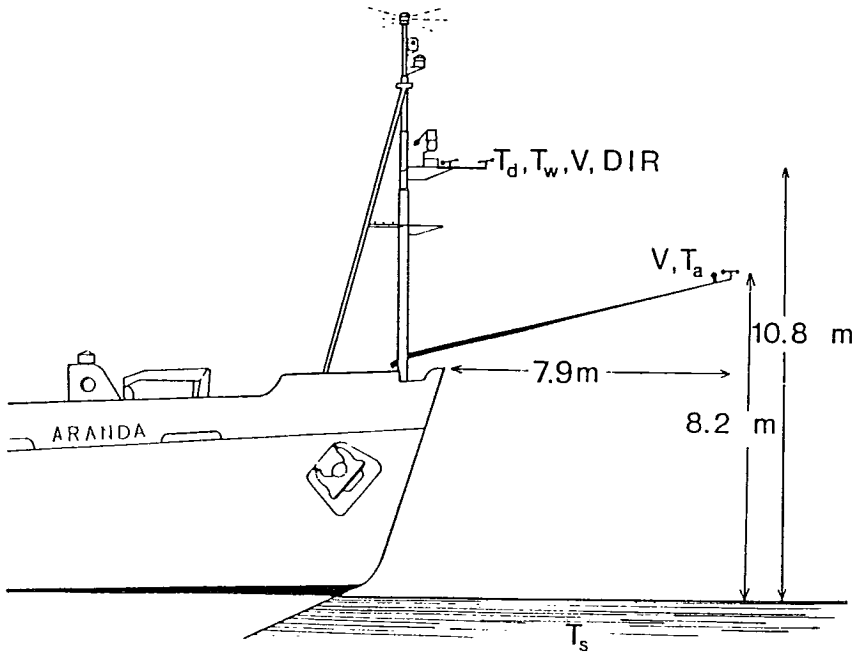

Fig. 2. Location of meteorological sensors on board R/V Aranda.

(velocity of 6.5 m/s) psychrometer system constructed for the ship at the Finnish Institute of Marine Research. During the experiment the system was calibrated regularly against an Assmann aspiration psychrometer, and the mutual differences were found to be insignificant; in average less than 1 % in terms of relative humidity or < 0.2 mb in water vapour pressure.

In addition to the quantities listed in Table 1, the data of which are available from the Øresund data bank (at Forskningscenter Risø, Denmark), observations were made about the cloudiness and the state of sea. A wave rider buoy was also moored, for determination of the characteristics of the waves and sea surface roughness, but the strong currents (> 0.4 m/s) in the shallow area badly distorted the data.

2.2 Calculation procedures

The turbulent fluxes of momentum (τ), sensible heat (H) and latent heat ($\mathcal{L}E$) were calculated by the familiar bulk formulae

$$\tau = \rho C_{Dz} V_z^2 \tag{1}$$

$$H = \rho c_p C_{Hz} (\theta_s - \theta_z) V_z \tag{2}$$

$$\pounds E = \pounds \rho C_{Ez} (q_s - q_z) V_z \tag{3}$$

where V_z is the mean wind speed at a height of z, ρ is the air density, c_p is the specific heat capacity of air and $\pounds$ is the enthalpy of vaporization. $\theta_s - \theta_z$ and $q_s - q_z$ are, the differences in potential temperature and specific humidity, between the atmosphere and the sea surface, respectively. The transfer coefficients, the drag coefficient C_{Dz}, Stanton number C_{Hz} and Dalton number C_{Ez}, may be expressed as

$$C_{Dz} = C_D(z, z_0, \Psi_M(z/L)) \tag{4}$$

$$C_{Hz} = C_H(z, z_0, z_T, \Psi_M(z/L), \Psi_H(z/L)) \tag{5}$$

$$C_{Ez} = C_E(z, z_0, z_q, \Psi_M(z/L), \Psi_E(z/L)) \tag{6}$$

where z is the measuring height and z_0, z_T and z_q are the roughness parameters for the wind speed, temperature and water vapour, respectively. L is the Monin-Obukhov length, and $\Psi_M(z/L)$ and $\Psi_H(z/L)$ and $\Psi_E(z/L)$ are the so-called universal functions which characterize the effects of the surface layer stability on turbulent transfer coefficients. (For further discussions of the bulk transfer coefficients see *e.g.* KONDO 1975, LAUNIAINEN 1979 and 1983, LARGE and POND 1982, BLANC 1985). In cases of the neutral stability, the transfer coefficients reduce to

$$C_{Dz} = C_D(z, z_0) \tag{7}$$

$$C_{Hz} = C_H(z, z_0, z_T) \tag{8}$$

$$C_{Ez} = C_E(z, z_0, z_q) \tag{9}$$

The universal functions and transfer coefficients are given in the functional form in Appendix 1.

GARRAT (1977) and WU (1980) have discussed and reviewed the drag coefficients over the sea surface. Now, because of the failure of our on-site wave measurements, there is hardly any other kind of physical standpoint for the basis of calculation of the flux of momentum than given by the studies mentioned. Therefore, a reasonable estimate for the neutral drag coefficient for the sea surface may be obtained from the data compilation formulae by either Garratt of Wu, the latter being somewhat more comprehensive. WU's (1980) wind dependent formula,

which was adopted for this study, reads

$$C_{D10N} \cdot 10^3 = 0.80 + 0.065\ V_{10} \tag{10}$$

where V_{10} is the wind speed at the height of 10 m. In fact, because of the limited fetches in the research area, this kind of approach may lead to an error in calculation of the flux of momentum, probably to an underestimation, the magnitude of which is extremely difficult to estimate (*cf.* WU 1980).

For the transfer coefficient of water vapour, a formula given by LAUNIAINEN (1983) was adopted, based on a relation of the coefficients of C_E/C_D, found in several data sets of eddy correlation results in literature. This formula reads

$$C_{E10N} = 0.63\ C_{D10N} + 0.32 \cdot 10^{-3} \tag{11}$$

If (10) is adopted for the drag coefficient, (11) gives

$$C_{E10N} \cdot 10^3 = 0.82 + 0.041\ V_{10} \tag{12}$$

which well agrees *e.g.* with a comprehensive data set by LARGE and POND (1982).

Furthermore, it is reasonable to assume that the water vapour and sensible heat transfer coefficients do not (*cf.* MONIN and YAGLOM 1977, LAUNIAINEN 1983) differ significantly from each other, *i.e.*

$$C_H \approx C_E \quad \text{or} \quad z_T \sim z_q \tag{13}$$

For the universal function (for a more detailed discussion see *e.g.* MONIN and YAGLOM 1977, DYER 1974, YAGLOM 1977, LAUNIAINEN 1979, VISWANADHAM 1982, BLANC 1985), such formulae were adopted that are most frequently used and experimentally tested; the so-called Webb-form for the stable region and Businger-Dyer form for the unstable region, given as (A5) and (A6) in Appendix 1.

The formulae (10) and (12) allow us, when V_{10} is known, to calculate the roughness lengths and the neutral transfer coefficients as (7) to (9) for any observation level. In diabatic cases the calculation of transfer coefficients of (4) to (6) and fluxes of (1) to (3) leads to an iterative solution of the system given as (A1) to (A6) in Appendix 1, (for a detailed description of the iteration procedure, see LAUNIAINEN 1979, p. 43). In addition, because the most reliable wind speed observations were obtained in this experiment from the bow sprit at the height of 8.2 m, the calculation of V_{10} was included in the iteration procedure, for getting the roughness parameters by using the formulae (10) and (12), as well as the correction of the specific humidity from the observation level of 10.8 m to

the calculation level of 8.2 m.

In addition to the flux quantities and the stability parameter, the friction velocity $v_\star$, defined as eq. (A1), was also calculated. The averaged (hourly) observations and calculated quantities are tabulated in Appendix 2.

3. *Results*

3.1 Temperature conditions

The beginning of the intensive period took part during the last part of a long-lasting sunny and calm early summer weather in the whole Scandinavia. By reason of this, *e.g.* the sea surface temperature in the Baltic Sea was 1 to 2 °C higher than normally and the mutual differences between (shallow) coastal and open sea areas were large.

Figure 3 shows the air-sea temperature conditions during 4 to 9 June and shows that most of the time the atmospheric surface layer was thermally stably stratified. The sea surface temperature was gradually increasing, whereas the air temperature, if the diurnal variation was filtered out, was decreasing. Accordingly, the degree of the thermal stability gradually decreased during the period.

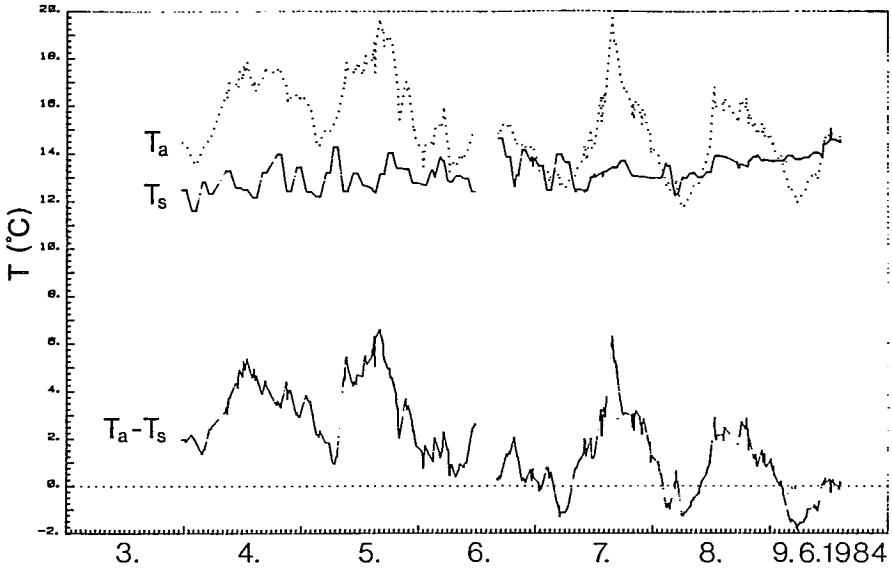

Fig. 3. Air temperature (T_a), sea surface temperature (T_s) and air-sea temperature difference in the Øresund area during 4th to 9th June 1984. (All single observations from the observation stations).

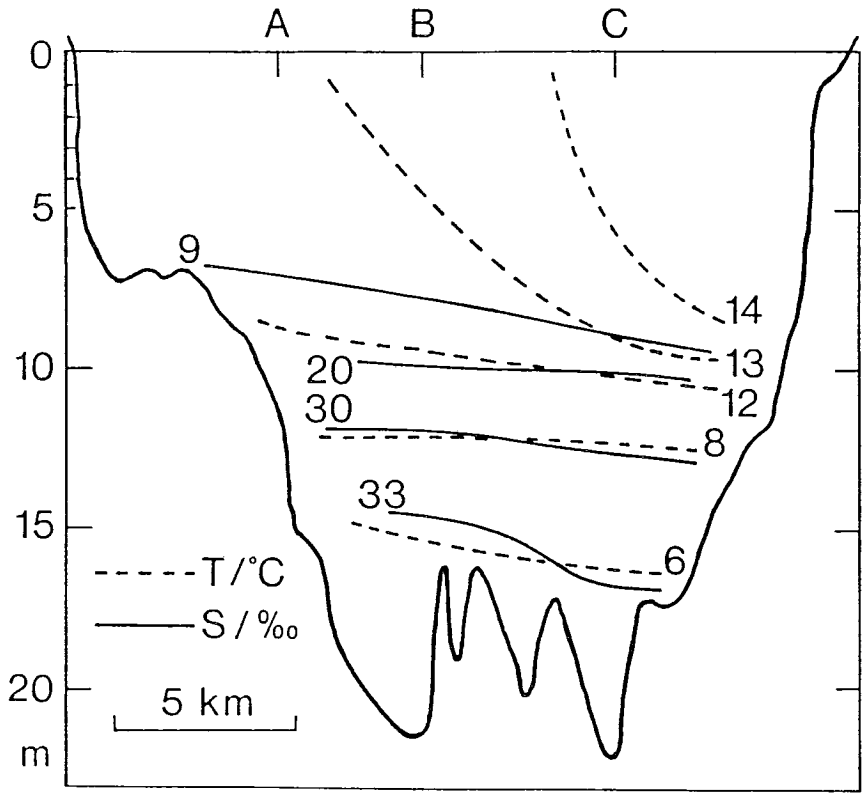

Fig. 4. Water temperature and salinity structure in a vertical section of the stations A–B–C for 5th June 1984.

Fig. 3 gives the general air-sea temperature conditions only. The time series of the sea surface temperature in Fig. 5 and also the average values for the period in Fig. 1b show that systematic (and oceanographically significant) areal differences existed in the sea surface temperature until 9th June. The sea surface was warmer on the eastern (Swedish) side than in the middle and on the western (Danish) side. The structure of water temperature and salinity in a vertical section of observation stations A to C (*cf.* Fig. 1b) for 5th June is given in Fig. 4. It shows a downward inclination of isotherms and isohalines toward the Swedish coast, characteristic of the period studied.

Oceanographically, the above kind of situation corresponds primarily to one where the warm and less saline Baltic surface water flows out from the Baltic Sea and the isohalines and isotherms indicate a geostrofic inclination, because the flow

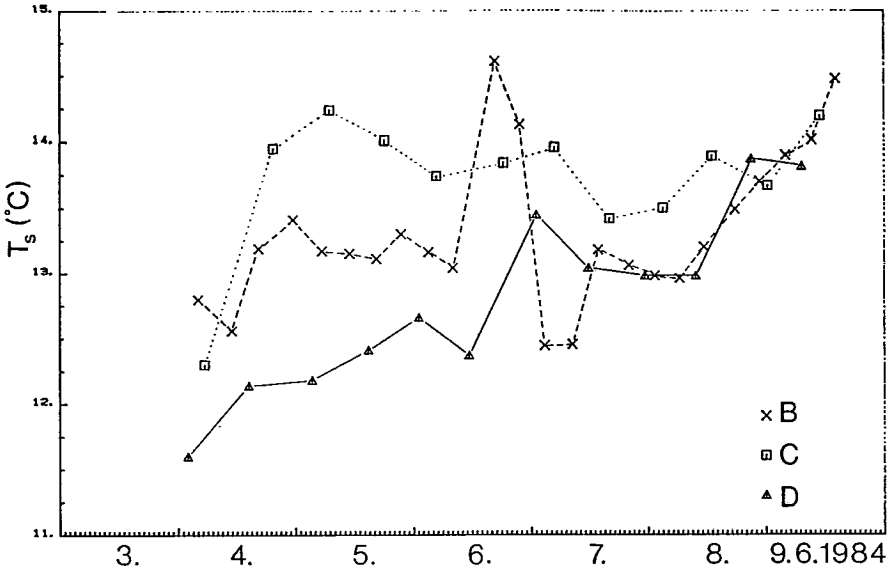

Fig. 5. Sea surface temperature at stations B, C and D during the intensive period. Station (hourly) averages.

can be considered to be only little affected by the local wind in this kind of a narrow channel. (The cross-sectional structure observed is well comparable to a theoretical situation in which an outflow, of the order of a half of the total outflow from the Baltic Sea, flows through the Øresund in the uppermost 8–9 m thick surface layer. The total outflow, for that time of year, may be estimated to be 25 000 – 30 000 m^3/s; *cf.* HUPFER *et al.*, 1979.) As a consequence of the differences in the sea surface temperature, corresponding differences may be found in atmospheric surface layer stability as well (*cf.* below).

3.2 Wind

The direction of the wind field during the period was rather stationary from between east and north, the vectorial average being of 63° (*cf.* Fig. 1b). The wind velocity decreased from moderate to very light during the period. The mean scalar wind speed is given in Fig. 6 as observed at the upwind and downwind observation sites of *C* and *D*, respectively. The results show that most of the time the surface wind speed was stronger at the upwind station. The maximum gusts observed (not given here) showed a similar behaviour. As to the areal differences, we can not find any reason in the experimental system for the above.

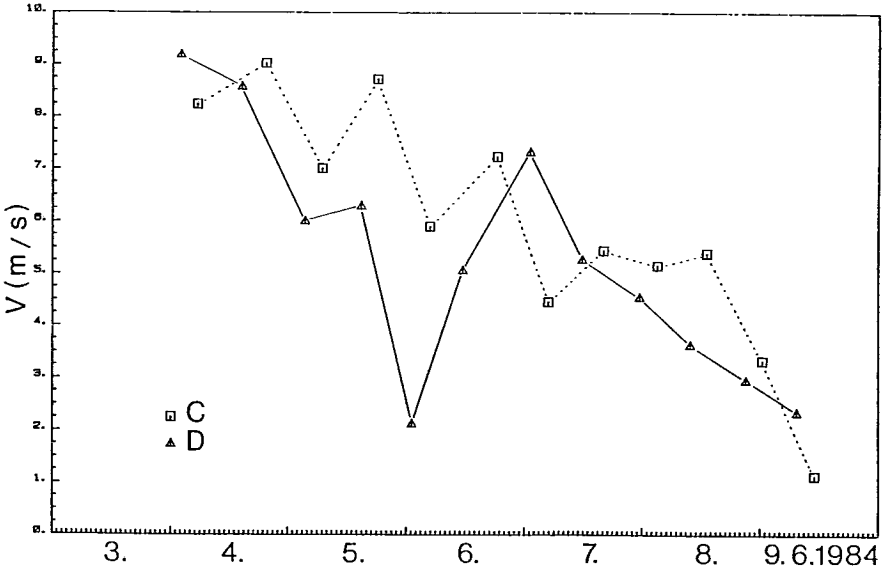

Fig. 6. Mean wind speed at the stations C and D. Station averages (of one hour).

3.3 Turbulent fluxes

Fig. 7 gives the time series of the momentum flux τ for the upwind and downwind stations considered. Owing to a lower wind speed and stronger stability (*cf.* Fig. 10), the momentum flux at the downwind stations seems to have been generally smaller than at the upwind station, indicating a similar anomalistic behaviour, if considered from the point of view of roughness and fetch only, as was found in the wind speed data discussed above. Especially, during the first three days, the differences in the momentum flux have been rather large.

The mutual upwind-downwind differences in the latent heat flux (evaporation), given in Fig. 8, were also rather large during the first few days of the intensive period. In the upwind area there was apparent evaporation, whereas in the downwind area evaporation was less significant and condensation was more frequent. This was due to the higher upwind sea surface temperature, the higher wind speed and the smaller upwind stability, whereas in the specific humidity in the air, controlling the vapour flux as well, no significant differences were found. The major role of the sea surface temperature is demonstrated in Fig. 8 in which also the latent heat flux is given as calculated for the upwind station data, but using the downwind observation as the sea surface temperature.

Though the mutual upwind-downwind differences appear in the wind conditions

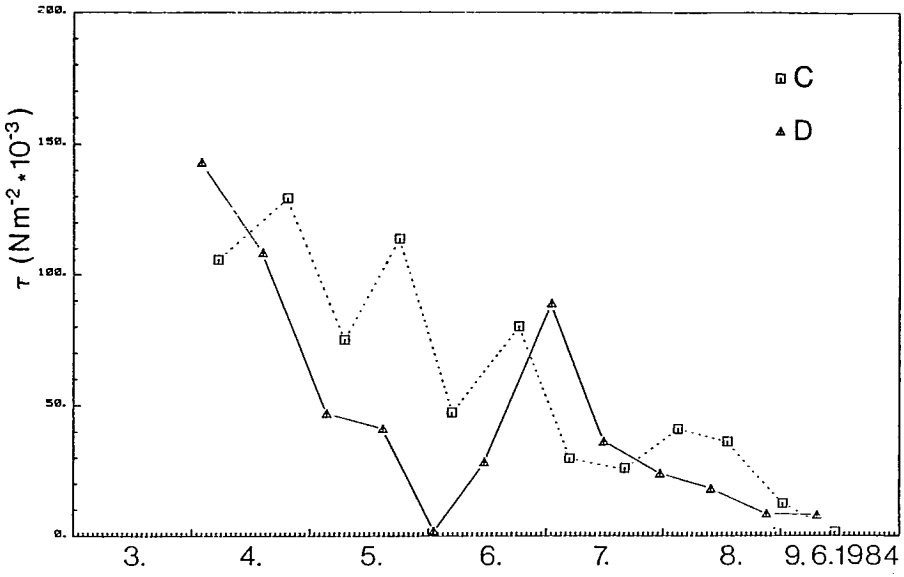

Fig. 7. Flux of momentum, τ (in mPa), at the stations C and D during 4th to 9th June 1984.

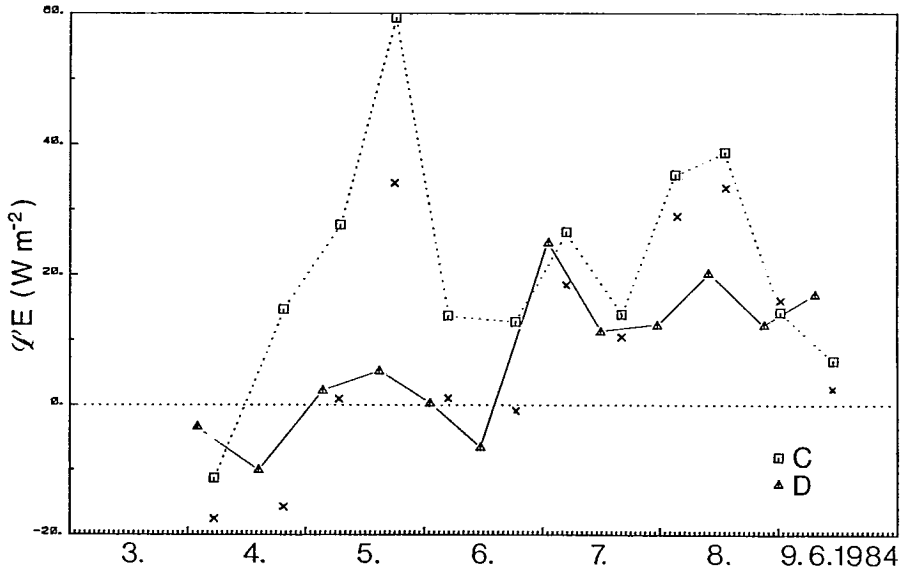

Fig. 8. Latent heat flux, $\mathcal{L}E$ (in Wm^{-2}), as calculated for the observation stations C and D. Small crosses (x) indicate the latent heat flux as calculated for the station C, but using as the sea surface temperature the values of the station D.

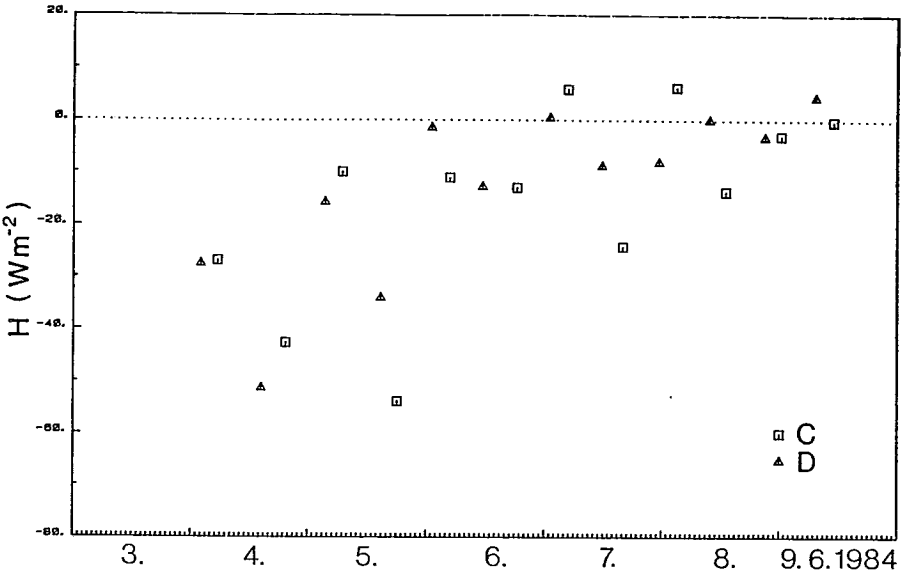

Fig. 9. Sensible heat flux, H (in Wm^{-2}), at the stations C and D.

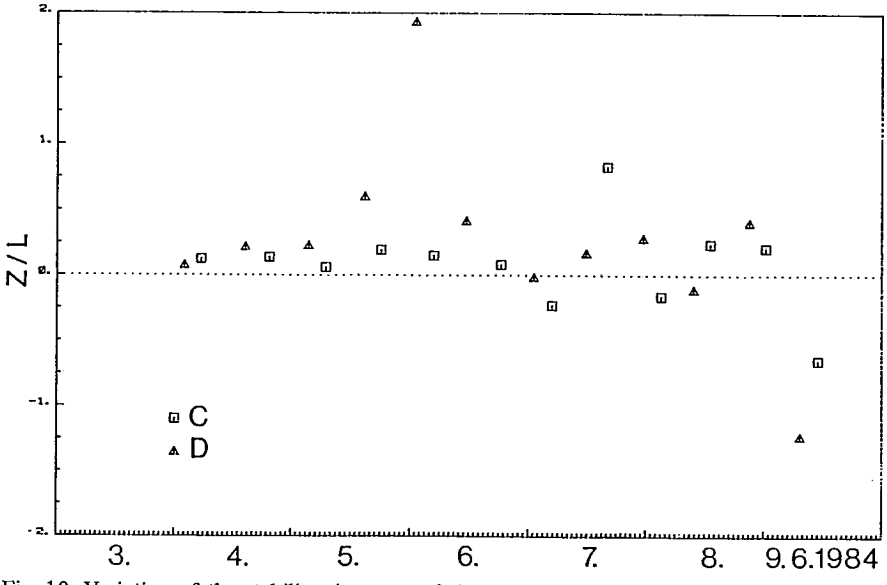

Fig. 10. Variation of the stability, in terms of the parameter z/L (z = 10 m), at the stations C and D during 4th to 9th June 1984.

and in the latent heat flux, it is interesting to find that in the sensible heat flux areal differences are not so apparent. For example, in the upwind area the larger wind velocity tends to increase the turbulent exchange, whereas in a stable case the higher sea surface temperature (smaller air-sea difference) diminishes the downward flux, and the final tendency is a combination of these effects. Additionally, small scale and diurnal variations in the air temperature cause variations in the sensible heat flux and make a mutual comparison of consecutive measurement stations difficult.

The surface layer stability is given in Fig. 10, in terms of the stability parameter z/L ($z = 10$ m). The results show, once again, that the upwind area was less stably stratified during the first days of the intensive period, mainly because of the higher upwind sea surface temperature and larger upwind velocity. At the end of the period, Fig. 10 shows very strong instability which is, however, due to the very small wind speeds, and thus of no practical importance.

4. *Discussion and conclusions*

Apparent areal and temporal variations in marine meteorological and air-sea exchange conditions during the intensive period of the Øresund-project were found in this study. The over-water surface wind speed and the flux of momentum were smaller at the downwind stations than at the upwind stations, most of the time. The upwind water vapour flux was larger as well, whereas in the sensible heat flux areal differences were not so apparent. Especially due to a higher sea surface temperature, also the atmospheric surface layer stability was less stable on the upwind (Swedish) side of the area.

When considering the above results, three physical standpoints connected with the study should be noticed. At first, the overall air-sea stratification in the area was rather stable most of the time. Secondly, horizontal differences in the sea surface temperature, wind speed and stratification existed in the area. Thirdly, diurnal variations were observed especially in the air temperature above the Øresund.

Although several theoretical approaches and laboratory experiments have been made (BRADLEY 1968, MULHEARN 1977, WOOD 1978, FOKEN and RAABE 1984), concerning the wind field modification due to a change in roughness, as well as some field tests (SETHURAMAN and RAYNOR 1980, LAUNIAINEN and SAARINEN 1982, KUZNECOV and RAABE 1985), only little attention has been given to accompanying effects of stability.

DORAN and GRYNING (1987) made an interesting study about the wind and temperature structure over a land-water-land area as scoped to the Øresund case.

They made a numerical model simulation of the development of the wind and temperature field for a case of 5 June 1984 noon. The model results suggested, in this rather stable case, the surface wind to accelerate over the water near the upwind coast (as a consequence of the change of roughness), to decelerate over the water fetch downwind and, finally to accelerate again as the second shore was encountered. The results were compared with the experimental data (few observations also from our data) and the agreement was good. In those results, a decrease in the surface wind velocity seems rather reasonable but, what was especially interesting, both in the simulation and in the observations, was that the downwards surface wind velocity over the water was lower than the upwind velocity above the solid land area. This means that, in this case, the stability effect decreasing the velocity, overstepped the roughness effect increasing the velocity. This is not generally assumed in studies of rough to smooth change. Actually, because of a flat upwind area, the upwind roughness and thus the coastal change in roughness was not very large in the area.

The over-water results of this study agree with the above scheme, and *e.g.* the variation in the upwind-downwind velocity difference (Fig. 6) corresponds to the general behaviour on the stability (Fig. 10) more of less, as does the momentum flux also in Fig. 7. Even in the average wind speeds (Fig. 1b) of our six days' period, this stability effect seems apparent. In fact, the air-sea difference diminished distinctly during the latter part of the period but so did also the wind speed.

DORAN and GRYNING (1987) discuss the wind field modification in the case, in terms of energy balance considerations for the atmospheric surface layer. The above may be considered, however, also with respect of water waves to be generated. In stable conditions the momentum flux, drawn by the waves from the atmosphere, cannot be as large as in the neutral case. In limited fetches this may, from the point of view of the waves, lead to an energy deficit and energy »suction» and decrease in the wind speed. This should be the case when the surface atmospheric layer stability increase with the fetch, as due to the decreasing sea surface temperature, as in this case. From the oceanographic point of view, however, a case in which the momentum flux decreases with the fetch, is of special interest.

As to the sensible and latent heat flux, especially the horizontal differences in the sea surface temperature, were found to play an important role. Together with the higher wind velocity, this resulted distinctly in larger upwind evaporation, whereas as to the sensible heat flux, these two effects tend to cancel the horizontal differences. In general, all the turbulent fluxes and air-sea exchange during the intensive period of this project were rather small, 20 to 60 % from the yearly averages in the open Baltic Sea, due to light winds and stable stratification.

During the study period diurnal variations were found, especially in the air temperature. This makes a strict quantitative upwind-downwind comparison difficult, because the observations were not carried out simultaneously at the stations to be compared. There was, however, no such kind of correlation between the diurnal variation and the time lag in the observation times, that might affect essentially the overall conclusions made.

Finally, the above data do not cover the areas close to the shoreline. As was shown *e.g.* by the satellite images, there existed a region (< 0.5 km) of warm shallow water near the coastline on both sides of the Øresund. In these narrow regions, the stability has been much less stable, even unstable in several cases (especially during the night-time), most probably. Accordingly, the flux conditions near the shoreline have different significantly from those in the open area, or moreover, they have been opposite in direction, as found *e.g.* over the Great Lakes and in the coast of the Gulf of Finland (LENSCHOW 1973, MCBEAN and PATERSON 1975, LAUNIAINEN and SAARINEN 1982).

Acknowledgements: The authors like to express their sincere thanks to captain Jukka Kyröhonka and the whole crew of the research vessel ARANDA, for arduous task in zigzagging in the busy Øresund area. The research program was carried out by an expedition, members of which were from Finnish Institute of Marine Research, University of Helsinki and completed by two voluntary Danish students.

The Øresund experiment was co-ordinated in practice by NORDFORSK (Nordic Co-operative Organization for Applied Research) and Dr. Sven-Erik Gryning (Risø Nat.laboratory, Denmark) is kindly acknowledged for the scientific co-ordination.

REFERENCES

BLANC, T.V., 1985: Variation of bulk-derived surface flux, stability and roughness results due to the use of different transfer coefficient schemes. – *J. Phys. Oceanogr.*, **15**, 650–669.

BRADLEY, E.F., 1968: A micrometeorological study of velocity profiles and surface drag in the region modified by a change in surface roughness. – *Quart. J.R. Met. Soc.*, **94**, 361–379.

DORAN, J.C. and S.-E. GRYNING, 1987: Wind and temperature structure over a land-water-land area. – *Journal of Climate and Applied Meteorology.* Submitted for publication.

DYER, A.J., 1974: A review of flux-profile relationships. – *Bound.-Layer Meteor.*, **7**, 363–372.

FOKEN, Th. and A. RAABE, 1984: Nahweis interner Grenzschichten im vertikalen Temperatur- und Feuchteprofil in der ufernahen Zone der Ostsee. – *Zeitschrift für Meteorologie*, **31**, 361–366.

GARRAT, J.R., 1977: Review of drag coefficients over oceans and continents. – *Mon. Wea. Rev.*, **105**, 915–929.

GRYNING, S.-E., 1985: The Øresund Experiment – A Nordic mesoscale dispersion experiment over a land-water-land area. – *Bull. Amer. Met. Soc.*, **66**, 1403–1407.

HUPFER, P., MIKULSKI, Z. and M. BÖRNGEN, 1979: Statistical analysis of river inflow to the Baltic Sea in the period 1921–1970. – *Sixth Meeting of Experts on the Water Balance of the Baltic Sea, International Hydrological Programme of the UNESCO,* 30.1.–2.2.1970 Hanasaari, Finland. 53 pp. (mimeogr.).

KONDO, J., 1975: Air-sea bulk transfer coefficients in diabatic conditions. – *Bound.-Layer Meteor.*, 9, 91–112.

KUZNECOV, O.A. and A. RAABE, 1985: Experimentelle Untersuchung der horizontalen Heterogenität des Windfeldes in der Kustenzone und Probleme ihrer theoretischen Beschreibung. – *Acta Hydrophysica, Heft 12/13,* 153–163.

LARGE, W.G. and A. POND, 1982: Sensible and latent heat measurements over the ocean. – *J. Phys. Oceanogr.*, **12**, 464–482.

LAUNIAINEN, J., 1979: Studies of energy exchange between the air and the sea surface on the coastal area of the Gulf of Finland. – *Finnish Marine Res.*, **246**, 3–110.

–»– , and J. SAARINEN, 1982: Examples of comparison of wind and air-sea interaction characteristics on the open sea and in the coastal area of the Gulf of Finland. – *Geophysica,* **19**, 33–46.

–»– , 1983: Parametrization of the water vapour flux over a water surface by the bulk aerodynamic method. *Annales Geophysicae,* **1**, 481–492.

LENSCHOW, D.H., 1973: Two examples of planetary boundary layer modification over the Great Lakes. – *J. Atmos. Sci.*, **30**, 568–581.

McBEAN, G.A. and R.D. PATERSON, 1975: Variations of the turbulent fluxes of momentum, heat and moisture over Lake Ontario. – *J. Phys. Oceanogr.*, **5**, 523–531.

MONIN, A.S. and A.M. YAGLOM, 1977: *Statistical Fluid Mechanics, Vol. 1.* The MIT Press, 769 pp.

MULHEARN, P.J., 1977: Relations between surface fluxes and mean profiles of velocity, temperature and concentration, downwind of a change in surface roughness. – *Quart. J.R. Met. Soc.*, **103**, 785–802.

SETHURAMAN, S. and G.S. RAYNOR, 1980: Comparison of mean wind speeds and turbulence at coastal site and an offshore location. – *J. Appl. Meteor.*, **19**, 15–21.

VISWANADHAM, Y., 1982: Examination of the empirical flux-profile models in the atmospheric surface bondary layer. – *Bound.-Layer Meteor.*, **22**, 61–77.

WOOD, D.H., 1978: Calculation of the neutral wind profile following a large step change in surface roughness. – *Quart. J.R. Met. Soc.*, **104**, 383–392.

WU, J., 1980: Wind stress coefficients over the sea surface near neutral conditions – A revisit. – *J. Phys. Oceanogr.*, **10**, 727–740.

YAGLOM, A.M., 1977: Comments on wind velocity and temperature flux-profile relationships. – *Bound.-Layer Meteor.*, **11**, 151–167.

APPENDIX 1. Formulae of flux-profile relationships (*cf.* Launiainen, 1983)

The turbulent fluxes of momentum, sensible heat and water are given as flux-profile relationships as

$$\begin{aligned}\tau &= \rho V_\star^2 = \rho k^2 \left[\ln \frac{z}{z_0} - \Psi_M(\zeta) \right]^{-2} V_z^2 \\ &= \rho C_{Dz} V_z^2\end{aligned} \tag{A1}$$

$$\begin{aligned}H &= \rho c_p k^2 \left[\ln \frac{z}{z_0} - \Psi_M(\zeta) \right]^{-1} \left[\ln \frac{z}{z_T} - \Psi_H(\zeta) \right]^{-1} (\theta_s - \theta_z)\, V_z \\ &= \rho c_p\, C_{Hz} (\theta_s - \theta_z)\, V_z\end{aligned} \tag{A2}$$

$$\begin{aligned}E &= \rho k^2 \left[\ln \frac{z}{z_0} - \Psi_M(\zeta) \right]^{-1} \left[\ln \frac{z}{z_q} - \Psi_E(\zeta) \right]^{-1} (q_s - q_z)\, V_z \\ &= \rho C_{Ez} (q_s - q_z)\, V_z .\end{aligned} \tag{A3}$$

where the stability parameter $\zeta = z/L$ is defined as

$$\zeta = \frac{z}{L} = -\frac{zgk\overline{w'\theta_v'}}{V_\star^3 T_0} = -\frac{zgkH(1 + 0.61\, T_0\, c_p E/H)}{V_\star^3 T_0 c_p \rho} . \tag{A4}$$

The formulae for the integrated universal functions, most frequently used and tested are:

– for the stable region ($\zeta > 0$)

$$\Psi_M = \Psi_H = \Psi_E = -\beta\zeta, \tag{A5}$$

the constant being $\beta \simeq 5$ (WEBB, 1970);

– for the unstable region ($\zeta < 0$) the BUSINGER *et al.* (1971) – DYER (1974) type form of

$$\left.\begin{aligned}\Psi_M &= 2\ln\left[\frac{1+\phi_M^{-1}}{2}\right]+\ln\left[\frac{1+\phi_M^{-2}}{2}\right]-2\,\overline{\text{arc tan}}\,\phi_M^{-1}+\pi/2\\ &\text{where}\\ \phi_M &= (1-\gamma\zeta)^{-1/4}\\ &\text{and}\\ \Psi_H &= \Psi_E = 2\ln\left[\frac{1+\phi_{HE}^{-1}}{2}\right],\\ &\text{where}\\ \phi_H &\approx \phi_E = (1-\gamma\zeta)^{-1/2} = \phi_M^2\end{aligned}\right\} \quad \text{(A6)}$$

the constant being γ = 15 to 16.

APPENDIX 2. Station averaged (hourly) observations and calculated quantities for 4 to 9 June 1984.

St	Date	Time (CET)	T_d	T_w	T_a	T_s	T_a-T_s	V	V_{10}	τ	H	$\mathcal{L}E$	$10/L$	q_z	$v_\star$
A	840603	2230-2320	14.45	12.70	14.43	12.46	1.97	10.37	10.595	194.74	-31.29	21.494	.053	8.447	.401
D	840604	0030-0120	13.69	12.56	13.64	11.60	2.04	9.20	9.394	142.98	-27.23	-3.160	.078	8.614	.343
B	840604	0240-0320	14.28	13.43	14.28	12.80	1.48	8.30	8.472	111.76	-17.30	-1.218	.071	9.262	.303
C	840604	0400-0440	14.82	13.72	14.70	12.30	2.40	8.24	8.410	105.71	-26.82	-11.26	.122	9.345	.295
E	840604	0730-0820	17.06	14.79	16.65	13.26	3.39	7.77	7.928	86.633	-33.24	-1.690	.197	9.575	.268
B	840604	0930-1020	17.41	14.96	17.01	12.56	4.45	7.17	7.314	65.462	-36.21	-10.28	.332	9.618	.233
A	840604	1100-1150	17.73	14.99	17.51	12.47	5.04	8.48	8.656	102.77	-53.35	-12.38	.248	9.520	.293
D	840604	1300-1350	17.03	14.44	16.79	12.14	4.65	8.59	8.769	108.34	-51.10	-9.877	.219	9.209	.300
B	840604	1500-1550	17.51	14.55	17.34	13.19	4.15	10.80	11.037	204.58	-66.39	12.330	.106	9.132	.413
C	840604	1800-1850	17.51	14.83	17.40	13.95	3.45	9.02	9.210	129.06	-42.61	14.725	.135	9.435	.328
E	840604	2000-2050	16.62	14.14	16.40	12.39	4.01	9.46	9.661	144.22	-52.52	-2.560	.145	9.055	.346
B	840604	2200-2250	16.55	14.08	16.18	13.41	2.77	9.19	9.384	138.91	-36.01	17.721	.101	9.020	.339
A	840605	0000-0050	16.19	13.97	16.04	12.38	3.66	7.75	7.908	85.172	-35.41	-1.899	.216	9.050	.266
D	840605	0200-0250	14.56	13.00	14.39	12.18	2.21	6.02	6.137	46.965	-15.57	2.359	.230	8.706	.197
B	840605	0400-0450	15.16	13.36	14.99	13.17	1.82	6.75	6.884	65.219	-15.65	12.490	.134	8.832	.232
C	840605	0530-0620	15.34	13.50	15.30	14.24	1.06	7.01	7.150	75.016	-10.03	27.645	.059	8.904	.249
E	840605	0730-0820	17.61	14.55	17.26	12.39	4.87	6.88	7.017	56.811	-36.07	-2.033	.403	9.091	.217
B	840605	0930-1020	17.89	14.77	17.53	13.15	4.38	7.24	7.386	67.924	-36.56	4.226	.308	9.215	.238
A	840605	1130-1220	18.10	14.57	17.75	12.62	5.13	7.33	7.478	67.653	-42.15	3.732	.358	8.914	.237
D	840605	1320-1410	18.41	14.38	18.12	12.41	5.71	6.31	6.434	41.158	-33.86	5.410	.602	8.584	.185
B	840605	1500-1550	19.43	14.10	19.24	13.11	6.13	9.50	9.702	137.32	-76.36	44.775	.215	7.871	.339
C	840605	1640-1730	18.92	13.78	18.77	14.01	4.76	8.72	8.902	113.56	-53.86	59.374	.194	7.741	.308
E	840605	1820-1910	16.49	13.39	16.23	13.36	2.87	4.03	4.104	13.504	-9.076	8.851	.812	8.323	.106
B	840605	2000-2050	17.00	13.48	16.73	13.30	3.43	4.27	4.349	14.795	-11.19	9.646	.879	8.208	.111
A	840605	2140-2230	15.07	13.11	14.91	12.74	2.17	3.17	3.226	6.770	-4.454	2.596	1.163	8.611	.075
D	840605	2340-0030	14.26	13.10	13.97	12.66	1.31	2.14	2.177	2.125	-1.277	.426	1.939	8.930	.042
B	840606	0140-0230	14.15	13.63	14.60	13.16	1.44	3.34	3.400	9.885	-4.059	-.539	.633	9.523	.090
C	840606	0320-0410	15.23	13.55	15.29	13.74	1.55	5.91	6.025	47.267	-11.18	13.721	.150	9.001	.198
E	840606	0500-0550	13.91	12.95	13.75	12.80	.95	7.85	8.010	99.534	-10.51	7.902	.048	8.920	.286
B	840606	0640-0730	13.64	12.72	13.64	13.04	.60	8.78	8.964	133.12	-7.830	17.791	.021	8.796	.331

cont.

St	Date	Time (CET)	T_d	T_w	T_a	T_s	T_a-T_s	V	V_{10}	τ	H	$\mathcal{L}E$	$10/L$	q_z	$v_\star$
A	840606	0820-0910	13.71	13.19	13.91	12.92	.99	7.53	7.683	89.415	-10.31	1.123	.058	9.246	.271
D	840606	1000-1050	14.78	13.85	14.84	12.37	2.47	5.08	5.176	28.286	-12.67	-6.371	.419	9.497	.153
B	840606	1520-1610	14.79	13.92	14.98	14.61	.37	6.89	7.027	74.298	-3.526	18.483	.016	9.567	.248
C	840606	1700-1750	15.17	13.83	15.18	13.84	1.34	7.25	7.396	80.047	-13.04	12.770	.081	9.318	.257
E	840606	1840-1930	14.29	13.58	14.47	12.91	1.56	6.27	6.393	54.496	-12.16	-2.371	.147	9.414	.212
B	840606	2020-2110	14.15	13.42	14.33	14.13	.20	6.00	6.117	54.132	-1.617	14.603	.007	9.305	.211
A	840606	2200-2250	14.05	13.19	14.16	13.72	.44	6.75	6.884	70.585	-4.076	15.173	.024	9.108	.241
D	840606	2340-0030	13.35	12.45	13.39	13.45	-.06	7.35	7.498	88.836	.638	25.023	-.014	8.642	.270
B	840607	0120-0210	13.08	11.78	13.05	12.44	.61	5.18	5.278	37.212	-3.990	14.267	.063	8.089	.175
C	840607	0320-0410	13.11	11.92	13.03	13.96	-.93	4.46	4.543	29.688	5.853	26.508	-.231	8.214	.156
E	840607	0500-0550	12.62	11.98	12.64	13.62	-.98	3.23	3.288	14.928	4.447	13.896	-.455	8.472	.111
B	840607	0700-0750	13.05	12.22	13.26	12.45	.81	4.25	4.328	22.218	-3.932	5.439	.164	8.535	.135
A	840607	0840-0930	14.12	12.58	14.00	12.42	1.58	4.57	4.655	24.033	-7.695	6.045	.297	8.460	.141
D	840607	1020-1110	14.49	12.86	14.42	13.04	1.38	5.29	5.391	36.195	-8.609	11.391	.172	8.592	.173
B	840607	1220-1310	16.35	13.63	16.07	13.18	2.89	3.62	3.685	9.008	-6.862	4.327	1.158	8.629	.086
C	840607	1440-1530	19.22	14.32	18.91	13.42	5.49	5.45	5.554	25.956	-24.18	13.946	.828	8.190	.147
E	840607	1620-1710	17.11	13.93	16.92	13.70	3.22	4.31	4.390	15.787	-11.08	8.886	.792	8.634	.115
B	840607	1840-1930	16.46	13.36	15.89	13.06	2.83	4.50	4.584	19.363	-11.36	9.851	.598	8.304	.127
A	840607	2020-2110	15.83	12.94	15.68	13.02	2.66	4.64	4.727	21.887	-11.66	12.337	.504	8.129	.135
D	840607	2200-2250	14.68	12.59	14.60	12.98	1.62	4.56	4.645	24.021	-7.903	12.398	.286	8.242	.141
B	840608	0000-0050	13.71	11.82	13.67	12.98	.69	4.64	4.727	28.565	-3.907	19.658	.079	7.873	.153
C	840608	0140-0230	12.67	11.18	12.65	13.50	-.85	5.16	5.258	40.892	6.252	35.310	-.162	7.675	.183
E	840608	0320-0410	12.23	10.98	12.45	12.28	.17	6.46	6.587	65.247	-1.528	26.907	-.003	7.663	.231
B	840608	0500-0550	11.98	10.47	11.76	12.96	-1.20	5.33	5.432	44.606	9.317	38.380	-.196	7.284	.191
A	840608	0640-0730	12.57	10.71	12.47	13.16	-.69	4.08	4.155	24.356	3.928	30.051	-.244	7.269	.141
D	840608	0820-0910	12.81	11.12	12.92	12.98	-.06	3.64	3.706	18.180	.285	20.363	-.108	7.561	.122
B	840608	1000-1050	14.09	11.57	14.03	13.20	.83	5.06	5.156	34.936	-5.230	29.898	.072	7.475	.170
C	840608	1140-1230	16.37	12.23	16.13	13.89	2.24	5.40	5.503	36.135	-13.67	38.703	.239	7.197	.173
E	840608	1320-1340	16.52	12.42	16.04	13.85	2.19	5.24	5.340	33.434	-12.78	34.871	.254	7.325	.166
B	840608	1620-1710	16.09	12.72	15.54	13.49	2.05	3.61	3.675	11.607	-6.248	12.820	.645	7.801	.098
A	840608	1800-1850	15.98	12.86	15.79	13.53	2.26	4.43	4.512	20.458	-9.720	16.734	.440	7.987	.130
D	840608	1940-2030	15.17	12.51	14.96	13.87	1.09	2.96	3.012	8.586	-3.023	12.390	.407	7.963	.084
B	840608	2120-2210	14.83	12.20	14.82	13.70	1.12	4.32	4.400	22.849	-5.494	23.036	.169	7.792	.137
C	840608	2300-2350	14.57	12.36	14.50	13.67	.83	3.33	3.390	12.485	-2.945	14.241	.210	8.057	.101
E	840609	0100-0150	13.75	11.79	13.67	13.69	-.02	1.78	1.810	4.077	.047	11.069	-.488	7.827	.058
B	840609	0240-0330	12.62	11.18	12.58	13.90	-1.32	2.62	2.666	9.962	5.081	20.819	-1.007	7.696	.090
A	840609	0420-0510	12.09	10.99	12.07	13.74	-1.67	2.96	3.012	12.972	7.334	22.288	-.923	7.729	.103
D	840609	0600-0650	12.43	11.27	12.51	13.82	-1.31	2.36	2.401	8.057	4.577	17.069	-1.223	7.859	.081
B	840609	0800-0850	13.03	11.63	13.09	14.02	-.93	2.09	2.126	6.176	2.833	15.060	-1.226	7.963	.071
C	840609	0940-1030	13.90	12.25	14.34	14.20	.14	1.14	1.159	1.616	-.207	6.793	-.649	8.219	.036
E	840609	1120-1210	14.78	13.03	14.74	14.62	.12	3.27	3.328	14.038	-.492	17.189	-.067	8.648	.108
B	840609	1300-1330	14.54	12.14	14.51	14.48	.03	3.01	3.063	12.058	-.117	23.015	-.175	7.850	.100

T_d = air temp. (dry) at 10.8 m in °C; T_w = wet bulb temp. at 10.8 m; T_a = air temp. at 8.2 m; T_s = sea surf. temp.; V = wind speed at 8.2 m in m/s; V_{10} = calculated wind speed for 10 m; τ = flux of momentum in $(N/m^2)*10^{-3}$; H = sensible heat flux in W/m^2; $\mathcal{L}E$ = latent heat flux in W/m^2; $10/L$ = stability; q_z = specific humidity in g/kg; $v_\star$ = friction velocity in m/s.

Positions: A: 55°47.5'N 12°41.1'E B: 55°47.8'N 12°45.0'E
C: 55°48.0'N 12°50.0'E D: 55°43.9'N 12°40.2'E